

# 1 Population diversity of cassava mosaic begomoviruses increases 2 over the course of serial vegetative propagation

3 Catherine D. Aimone<sup>1</sup> and Erik Lavington<sup>2</sup>, J. Steen Hoyer<sup>2</sup>, David O. Deppong<sup>1</sup>, Leigh  
4 Mickelson-Young<sup>1</sup>, Alana Jacobson<sup>3</sup>, George G. Kennedy<sup>4</sup>, Ignazio Carbone<sup>4</sup>, Linda Hanley-  
5 Bowdoin<sup>1</sup>, Siobain Duffy<sup>2\*</sup>

## 7 **Author affiliations**

8 <sup>1</sup>Department of Plant and Microbial Biology, North Carolina State University, Raleigh NC  
9 27695 USA

10  
11 <sup>2</sup>Department of Ecology, Evolution, and Natural Resources, Rutgers University, New  
12 Brunswick, NJ 08901 USA

13  
14 <sup>3</sup>Department of Entomology and Plant Pathology, Auburn University, Auburn, AL 36849 USA  
15

16 <sup>4</sup>Center for Integrated Fungal Research, Department of Entomology and Plant Pathology, North  
17 Carolina State University, Raleigh NC 27695 USA  
18

19 \*Correspondence: Siobain Duffy, [duffy@sebs.rutgers.edu](mailto:duffy@sebs.rutgers.edu)

20 **Keywords:** cassava mosaic begomoviruses, viral diversity, vegetative propagation

21 **Abbreviations:** ACMV, African cassava mosaic virus; EACMCV, East African cassava mosaic  
22 Cameroon virus; CMD, Cassava mosaic disease; CMB, Cassava mosaic begomovirus; PTGS,  
23 Post-transcriptional gene silencing; TGS, Transcriptional gene silencing; ssDNA, Single-  
24 stranded DNA; dsDNA, Double-stranded DNA; RCA, Rolling circle amplification; CP, Coat  
25 protein; Rep, Replication-associated protein; REn, Replication enhancer protein; MP, Movement  
26 protein; NSP, Nuclear shuttle protein; SEGS, Sequence enhancing geminivirus symptoms.

27 **Repositories:** - Veg2: PRJNA667210 and Veg6: PRJNA658475  
28

29

30 **Abstract**

31 Cassava mosaic disease (CMD) represents a serious threat to cassava, a major root crop for more  
32 than 300 million Africans. CMD is caused by single-stranded DNA begomoviruses that evolve  
33 rapidly, making it challenging to develop durable disease resistance. In addition to the  
34 evolutionary forces of mutation, recombination, and reassortment, factors such as climate,  
35 agriculture practices, and the presence of DNA satellites may impact viral diversity. To gain  
36 insight into the factors that alter and shape viral diversity *in planta*, we used high-throughput  
37 sequencing to characterize the accumulation of nucleotide diversity after inoculation of  
38 infectious clones corresponding to African cassava mosaic virus (ACMV) and East African  
39 cassava mosaic Cameroon virus (EACMCV) in the susceptible cassava landrace Kibandameno.  
40 We found that vegetative propagation had a significant effect on viral nucleotide diversity, while  
41 temperature and a satellite DNA did not have measurable impacts in our study. EACMCV  
42 diversity increased linearly with the number of vegetative propagation passages, while ACMV  
43 diversity increased for a time and then decreased in later passages. We observed a substitution  
44 bias toward C→T and G→A for mutations in the viral genomes consistent with field isolates.  
45 Non-coding regions excluding the promoter regions of genes showed the highest levels of  
46 nucleotide diversity for each genome component. Changes in the 5' intergenic region of DNA-A  
47 resembled the sequence of the cognate DNA-B sequence. The majority of nucleotide changes in  
48 coding regions were non-synonymous, most with predicted deleterious effects on protein  
49 structure, indicative of relaxed selection pressure over 6 vegetative passages. Overall, these  
50 results underscore the importance of knowing how cropping practices affect viral evolution and  
51 disease progression.

52 **Introduction**

53 Begomoviruses (genus *Begomovirus*, family *Geminiviridae*) are single-stranded DNA (ssDNA)  
54 viruses that cause serious diseases in many important crops worldwide (1). They are  
55 characterized by their double icosahedral particles and whitefly (*Bemisia tabaci* Genn) vectors  
56 (2, 3). Like other ssDNA viruses (4-9), begomoviruses have the potential to evolve rapidly  
57 because of their small genomes, large population sizes, short generation times, and high  
58 substitution rates (10, 11). Begomoviruses also readily undergo recombination (12), but mutation  
59 is the major driver of diversification of begomovirus populations (13, 14). The highly  
60 polymorphic nature of begomovirus populations can lead to rapid adaptation and increased  
61 virulence (15, 16). Plant virus evolution is also influenced by ecological conditions, such as  
62 agricultural practices and environmental stresses (17-20).

63  
64 Cassava is a major root crop in Africa (21), whose production has been severely impacted by a  
65 rapidly evolving complex of 11 begomoviruses species, 9 of which are in Africa, which cause  
66 Cassava mosaic disease (CMD) (22). Cassava mosaic begomoviruses (CMBs) have bipartite  
67 genomes that consist of two circular DNAs designated as DNA-A and DNA-B (23). Both  
68 genome components, which together are ca. 5.5 Kb in size, display high nucleotide substitution  
69 rates of approximately  $10^{-3}$  to  $10^{-4}$  substitutions per site per year (10), which are similar to the  
70 rates reported for RNA viruses (24, 25). DNA-A is necessary for viral replication, transcription  
71 and encapsidation, while DNA-B is required for viral movement (2, 3). Both genome  
72 components contain divergent transcription units separated by a shared 5' intergenic sequence or  
73 common region that contains the origin of replication and promoters for viral gene transcription  
74 (2, 3). The viral replication origin includes a hairpin structure that contains the nick site for

75 rolling circle replication and iteron motifs that function as origin recognition sequences (26, 27).  
76 The origin motifs are conserved between cognate DNA-A and DNA-B components.  
77  
78 DNA-A encodes six proteins via overlapping genes, while DNA-B encodes two proteins on  
79 nonoverlapping genes (2, 3). (See Supplementary Figure 1 for diagrams of viral clones and major  
80 functions of the viral proteins). Genes specified on the complementary DNA strand are  
81 designated as “C”, while genes on the virion strand are indicated as “V”.) The replication-  
82 associated protein (Rep, *AC1*), which catalyzes the initiation and termination of rolling circle  
83 replication (28) and functions as a DNA helicase (29), is the only viral protein essential for  
84 replication (30). REn (*AC3*) greatly increases viral DNA accumulation by facilitating the  
85 recruitment of host DNA polymerases for viral replication (31). Viral ssDNA generated during  
86 rolling circle replication can be converted to dsDNA (32) and reenter the replication cycle or be  
87 packaged into virions composed of the coat protein (CP, *AVI*) (33). TrAP (*AC2*) is a  
88 transcription factor (34). TrAP, *AC4*, and *AV2* counter host defenses by interfering with post-  
89 transcriptional gene silencing (PTGS) and transcriptional gene silencing (TGS) (for review  
90 see(35). ACMV DNA-A also includes an *AC5* ORF of unknown function that overlaps *AVI* (36,  
91 37). DNA-B encodes two proteins essential for movement. The movement protein (MP, *BC1*) is  
92 necessary for viral transport through the plasmodesmata into adjacent cells and systemically  
93 through the plant (38, 39). The nuclear shuttle protein (NSP, *BVI*) is involved in viral DNA  
94 trafficking into and out the nucleus and across the cytoplasm to the cell periphery in coordination  
95 with MP (38-40).

96



97 CMBs often occur in mixed infections leading to synergy between the coinfecting viruses and  
98 increased symptom severity (12, 41). In the 1990s and 2000s, synergy between *African cassava*  
99 *mosaic virus* (ACMV) and a recombinant CMB contributed to a severe CMD pandemic that  
100 spread from Uganda to other sub-Saharan countries and devastated cassava production (12, 42).  
101 In response to the pandemic, many African farmers adopted cassava cultivars with the CMD2  
102 locus, which confers resistance to CMBs (43, 44). Cassava plants displaying severe, atypical  
103 CMD symptoms were observed in some fields after the widespread adoption of CMD2-resistant  
104 cultivars (45). Subsequently, two DNAs, SEGS-1 and SEGS-2 (sequences enhancing  
105 geminivirus symptoms), were shown to produce similar symptoms when coinoculated with  
106 CMBs into both resistant and susceptible cassava cultivars (45). SEGS-2, which occurs as  
107 episomes in CMB-infected cassava, virions and whiteflies, is thought to be a novel satellite (46).  
108 SEGS-1 also forms episomes in CMB-infected cassava but is likely derived from a cassava  
109 genomic copy (45). The uniqueness of SEGS-1 and SEGS-2 raises questions about how they  
110 interact with other viral components and might impact begomovirus diversity.

111  
112 Little is known about how vegetative propagation, environmental factors, and the presence of the  
113 SEGS affect CMB evolution. To generate knowledge about the impact of these factors, we  
114 examined viral diversity in mixed infections of ACMV and *East African cassava mosaic*  
115 *Cameroon virus* (EACMCV) during serial vegetative propagation of cassava plants inoculated  
116 with only CMBs or coinoculated with SEGS and grown under controlled conditions at two  
117 temperatures. This study provided evidence that vegetative propagation, but not temperature or  
118 the presence of SEGS, had a significant impact on viral diversity over time.

119

120 **Methods**

121 **Vegetation Propagation Study with Two Passages (Veg2) at Two Temperatures**

122 Cassava plants (*Manihot esculenta* cv. Kibandameno) were propagated at 28°C and 30°C under a  
123 12-h light/dark cycle representing the predicted 2°C temperature shift in Africa by 2030 (47) and  
124 inoculated using a microsyringe to deliver plasmids (100 ng) containing partial tandem dimers of  
125 DNA-A or DNA-B of ACMV (Accession Numbers: MT858793.1 and MT858794.1) and  
126 EACMCV (Accession Numbers: MT856195 and MT856192) (48, 49). Three plants were  
127 coinoculated with ACMV and EACMCV clones for each temperature treatment with each plant  
128 representing a biological replicate. Samples (1 mg) were collected at 28 days post inoculation  
129 (dpi) from symptomatic tissue near the petiole of leaf 2 (relative to the plant apex), flash-frozen  
130 in liquid nitrogen, and stored at -80°C until analysis. At 56 dpi, a stem cutting with two nodes  
131 was generated from each biological replicate and transferred to fresh soil after treatment with  
132 rooting hormone (Garden Safe: TakeRoot Rooting Hormone). The stem cuttings were sampled at  
133 28 days after propagation as described above and used for the next round of propagation at 56  
134 days. Propagated plants originating from the same inoculated source plant represent a lineage.  
135 Leaf tissue collection and propagation continued for a total of two rounds at each temperature  
136 following the above protocol. Frozen leaf tissue was ground, total DNA was extracted using the  
137 MagMax™ Plant DNA Isolation Kit (Thermo Fisher Scientific, Waltham, MA), and DNA < 6  
138 Kb in size was selected using the Blue Pippin Prep system (Model # BDQ3010, Sage Science,  
139 Beverly MA) prior to library prep (50).

140 **Vegetative Propagation Study with Six Passages (Veg6)**

141 Kibandameno plants were propagated from stem cuttings, grown at 28°C, and inoculated as  
142 described above. Plants were inoculated with plasmid DNA (100 ng) corresponding to ACMV +

143 EACMCV, ACMV + EACMCV + SEGS-1 (AY836366), or ACMV + EACMCV + SEGS-2  
144 (AY836367). Each treatment was replicated 3 times. Leaf samples were collected, and stem  
145 cuttings were propagated as described above. This process was repeated six times with a total of  
146 seven rounds including the initial inoculated plant. Total DNA was isolated but was not size-  
147 fractionated because earlier serial experiments showed that sequencing total DNA samples  
148 produce sufficient read coverage for viral diversity analysis (50).

### 149 **Library Preparation**

150 Sequencing libraries for Veg2 and Veg6 were generated using EquiPhi polymerase (Thermo  
151 Fisher Scientific, Waltham MA) for rolling circle amplification (RCA) and the Nextera XT kit  
152 (Illumina, San Diego CA) with unique dual index sequences for library preparation (50). The  
153 protocol was modified to include two RCA reactions for each sample. Each RCA reaction was  
154 diluted to 5 ng/mL, and 2  $\mu$ L of each reaction were combined. The combined RCA reactions  
155 were diluted to 0.2 ng/ $\mu$ L (1 ng total in 5  $\mu$ L) and used to construct two technical replicate  
156 libraries. Libraries of the inoculum plasmids for ACMV and EACMCV (1 ng of plasmid DNA in  
157 5  $\mu$ L) were also prepared using the Nextera XT kit. The libraries were pooled in equimolar  
158 amounts and sequenced on an Illumina NovaSeq 6000 S4 lane to generate 150-bp, paired-end  
159 reads.

### 160 **Analysis of Raw Reads**

161 Raw sequencing data were processed according to Aimone et al. (2020); the workflow is also  
162 available on Galaxy (ViralSeq, <https://cassavavirusevolution.vcl.ncsu.edu/>). Raw Illumina data is  
163 available from the NCBI Sequence Read Archive for Veg2 (PRJNA667210) and Veg6  
164 (PRJNA658475).

### 165 **SNP filtering and functional analysis**

166 SNPs were detected using VarScan (51) and filtered for all SNPs present in both of the  
167 sequencing technical replicates and at a frequency  $\geq 3\%$  in at least one replicate. SNPs present at  
168  $\geq 3\%$  frequency in both technical replicates and present in more than one passage were selected  
169 for functional analyses. SNPs were categorized by intergenic region, protein, functional domain,  
170 and known motif using SNPeff (52). SNPs in coding regions were categorized as synonymous or  
171 non-synonymous. The SIFT tool D algorithm was used to predict the effects of single amino acid  
172 substitutions caused by non-synonymous codons, with a substitution scored as damaging ( $\leq 0.05$ )  
173 or tolerated ( $> 0.05$ ) (53). Predictions are based on a scaled probability matrix built by the SIFT  
174 algorithm using protein sequence alignments between the queried protein sequence and proteins  
175 in known databases, in this case [non-redundant protein] (53). In the overlaps between coding  
176 regions, if a SNP was called using VarScan and identified by protein region using SNPeff in one  
177 coding region, its impact on the second coding region was categorized as synonymous or non-  
178 synonymous. SNPs in the common regions of the DNA-A and DNA-B of ACMV or EACMCV  
179 were compared to one another and the reference sequence of the infectious clone for each viral  
180 genome component used in the propagation studies. The alignments were performed using a  
181 Smith-Waterman sequence alignment (54) using SnapGene software (from Insightful Science;  
182 available at [snapgene.com](http://snapgene.com)). A Mann-Whitney Test in R was used to calculate the difference  
183 between the frequency of SNPs observed in the historical database and SNPs that occurred in  
184 Veg6 experiment.

### 185 **Nucleotide diversity and Tajima's D**

186 Nucleotide diversity was calculated from SNP frequencies per nucleotide position by the formula  
187  $\pi = \sum_{ij} x_i x_j \pi_{ij}$  (55) using custom Python scripts. When calculating Tajima's D, total read  
188 coverage averaged across all SNPs for a given region was used as a proxy for sample size (56).

189 Sliding window calculations of  $\pi$  were calculated by custom Python scripts with a window size  
190 of 300 bp and a step of 10 nucleotides and are reported at the central position of the window.

### 191 **Experimental effect analyses**

192 The effect size of experimental design variables was analyzed in Python by linear regression  
193 using the statsmodels module (v0.12.0) with genomic nucleotide diversity as the response (57).  
194 Details of the model and results are discussed below.

### 195 **Analysis of nucleotide substitution bias**

196 Filtered SNPs were combined by experiment, species, and component across all passages. Each  
197 unique substitution was used to generate observed counts. Substitution counts for each pair of  
198 nucleotides were tested by a  $\chi^2$  test of independence on a 2X2 contingency table of observed and  
199 expected counts. To generate the expected counts for each pair, we assumed that substitutions in  
200 both directions were equally likely, divided observed counts in half, and adjusted for nucleotide  
201 proportions in the reference sequence (10). For example, considering the test for A $\leftrightarrow$ T  
202 substitution bias in ACMV DNA-A in the Veg2 experiment, we observed a total of 5 A $\rightarrow$ T and  
203 13 T $\rightarrow$ A substitutions. Counts of A and T in the ACMV DNA reference are 743 and 795,  
204 respectively, yielding expectations of 8.7 A $\rightarrow$ T and 9.3 T $\rightarrow$ A.

### 205 **Data and analysis availability**

206 Data in the form of VarScan outputs for each of the models with associated metadata along with  
207 custom scripts used for analyses are available at <https://www.github.com/elavington/PIRE>.

208

## 209 **Results**

### 210 **Experimental variable effects**

211 We tested the effects of three treatments (temperature, vegetative propagation, and the presence  
212 of SEGS) on nucleotide diversity of ACMV and EACMCV in two experiments designated as  
213 Veg2 and Veg6. Veg2 tested the effect of temperature and included bombard plants (Passage 1,  
214 P1) and plants from two rounds of propagation (P2 and P3). Veg6 included clonally bombard  
215 plants (P1) and six subsequent rounds of propagation (P2-P7) that tested the effect of SEGS  
216 presence and vegetative propagation. Each experiment was conducted with three bioreplicates  
217 (independently inoculated plant lineages) per treatment. Best fit linear regression models  
218 included passage rounds, viral species (ACMV and EACMCV), and segment (DNA-A or DNA-  
219 B) nested in species (Tables 1 and 2, full experimental models are included in Tables S1 and S2.)  
220 Given the lack of evidence for a significant effect for several experimental treatments (replicate,  
221 temperature, and SEGS) and the failure of the full model to pass diagnostic tests of normality  
222 (Jarque-Bera test) and autocorrelation (Durbin-Watson test) (58), we grouped samples by  
223 generating a mean variant frequency. For example, to group SEGS treatments (no SEGS, +  
224 SEGS-1, + SEGS-2), we averaged allele frequencies across all three SEGS treatments for each  
225 SNP that shared the same passage, species, segment, and lineage. This had the effect of reducing  
226 the number of samples while generating a data set and model that passed diagnostic tests. Sample  
227 grouping consistent with this model was used for the rest of the analyses presented in this study.  
228 Both Veg2 and Veg6 grouped data were fit to the model:

$$y = \alpha + R_i + S_j + S_j(G_k) + \varepsilon_{ijk}$$

229  
230 With  $R$  for the initial bombardment and each  $i$ th passage number,  $S$  for species,  $G$  for segment  
231 nested in species, intercept  $\alpha$  and error term  $\varepsilon$ . The overall models were significant for both  
232 Veg2 ( $p = 0.00115$ ,  $R^2 = 0.834$ ) and Veg6 ( $p = 0.00537$ ,  $R^2 = 0.438$ ). Only passage was

233 significant in both Veg2 and Veg6, accounting for 94% and 79% of the variance explained by  
234 the model, respectively (as eta-squared calculated from Tables 1 and 2).

### 235 **Viral diversity changes over time**

236 After determining that passage number (P1-P3 for Veg2; P1-P7 for Veg6) was the only factor  
237 that significantly impacted viral diversity quantitatively, we investigated how the diversity  
238 changed through successive rounds of vegetative propagation across the ACMV and EACMCV  
239 genome components. Sliding windows of  $\pi$  were calculated across segments accounting for their  
240 circular architecture and information retained after grouping read counts.  $\pi$ , which is the average  
241 pairwise difference between sequences in a sample (55), was examined on a population level and  
242 not by plant lineage, due to lineage failing to pass the test of normality and autocorrelation  
243 (Tables S1 and S2). Maximum  $\pi$  values were higher in the Veg6 experiment than the Veg2  
244 experiment, suggesting that more rounds of vegetative propagation allowed for greater  
245 accumulation of nucleotide diversity (cf. Fig. 1 and 2). Comparison of P1, P2 and P3 between  
246 Veg2 and Veg6 revealed that the patterns of diversity are similar (Fig. 1a and c; S2a and c),  
247 except for a decrease in  $\pi$  in the ACMV *AVI* gene at P3 of Veg6 (cf. Fig. 1b and S2b). The  
248 patterns of increasing and decreasing  $\pi$  along genome components varied across passages, with  
249 several regions increasing in diversity across passages in Veg6 (Fig. S2a and S2c). Variation  
250 along the genome components was most apparent for EACMCV, which showed the highest level  
251 of nucleotide diversity in P7 for both genome components (Fig. 1c and S2c). The nucleotide  
252 diversity for EACMCV-A at P6 was intermediate between that of P7 and P4/P5, and the  
253 diversity of EACMCV-B was similar for P4-P6. In contrast, both genome components of ACMV  
254 displayed the highest levels of diversity at P4 and P6, with P5 and P7 showing lower levels (Fig.  
255 2a and S2a).

256

257 The DNA-A components of ACMV and EACMCV exhibited similar patterns of diversity in the  
258 passages showing the highest levels of nucleotide diversity, i.e., P4 for ACMV and P7 for  
259 EACMCV in the V6 experiment (Fig. 2a and c). The highest peaks of nucleotide diversity were  
260 over *AV2* and *AVI* (Fig. 2a and c). In ACMV-A, nucleotide diversity covered a broader region of  
261 *AVI* overlapping with *AC5* encoded on the opposite strand. Peaks of diversity were also  
262 observed over other overlapping regions of ACMV-A: *AC1/AC4* and *AC2/AC3* (Fig. 2a and 2b).  
263 In EACMCV, two peaks of diversity occurred over non-overlapping coding regions of *AC1*, with  
264 overlapping regions showing moderate diversity (Fig. 2c and 2d). It was unexpected that  
265 nucleotide diversity appeared to peak in regions where viral genes overlap in different reading  
266 frames, in which codon wobble positions would be constrained. Chi-square tests confirmed that  
267 diversity was not constrained by the number of overlapping protein coding regions within  
268 ACMV-A or EACMCV-A ( $p > 0.21$ , Table S3-3). The DNA-B components of ACMV and  
269 EACMCV also displayed similar patterns of nucleotide diversity (Fig. 2a and 2c). High levels of  
270 diversity were seen in the 5' intergenic region, and *BCI* had higher levels compared to *BVI*.

### 271 **Test of evolution/demographic changes**

272 After examining viral diversity on the genomic level, we examined the potential impact of more  
273 frequent individual variants. We examined the effect of varying minimum variant frequency  
274 thresholds on Tajima's D, which infers selection and/or demographic events (population size  
275 changes not due to selection) and is sensitive to rare variants (59). Tajima's D is the standardized  
276 difference of two different ways to calculate the expected nucleotide diversity. The caveat with  
277 using Tajima's D is that purely demographic changes in the population can result in extreme  
278 values of Tajima's D. Our study has an advantage to this point over the problem of disentangling



279 selection and demographic histories in wild populations: given our experimental design we have  
280 a good understanding of what demographic effects are possible. We also do not use dN/dS as this  
281 measure is not well suited to the short evolutionary time frame and likely small population sizes  
282 found in these experiments. We filtered SNPs by varying the minimum frequency for each of the  
283 Veg2 and Veg6 experiments (Fig. 3). In Fig. 3, SNP frequencies were grouped by passage and  
284 segment nested within species (ACMV-A, ACMV-B, EACMCV-A, EACMCV-B) for each  
285 experiment. General interpretations of Tajima's D typically hold for minimum variant  
286 frequencies of 2-4% for SNP analysis (59). Hence, we used a minimum variant frequency of 3%  
287 in our analysis (Fig. 3, dotted vertical line) to rule out the influence of very rare variants and  
288 simplify the analysis of potential functional implications of variance. In the Veg2 experiment,  
289 Tajima's  $D > 2$  was significant ( $P < 0.01$ ) in P2 for ACMV DNA-B and in P3 for ACMV DNA-A,  
290 ACMV DNA-B, and EACMCV DNA-B (Fig. 3a and b), but not for EACMCV DNA-A in any  
291 passage (Fig. 3b). In contrast, the later passages of the Veg6 experiment were positively  
292 significant for all segments (Fig. 3c and d), but the magnitudes of Tajima's D for all segments  
293 varied across passages in a nonlinear fashion similar to the nucleotide diversity profiles (Fig. S2).  
294 The marginal significance ( $0.01 < P < 0.05$ ) of a positive Tajima's D in the Veg2 and Veg6  
295 experiments indicates more intermediate-frequency variants than expected and does not support  
296 strong selective sweeps in either experiment. We note our data do not support strong selective  
297 sweeps or detectable population bottlenecks even though our methods are not as conservative as  
298 those in other pool-seq genetic diversity analytics (56).

### 299 **Biases in nucleotide substitutions**

300 High mutation rates of ssDNA viruses have been attributed to deamination and oxidative damage  
301 (10, 60). Thus, we investigated whether nucleotide substitution bias was detectable within the

302 timeframe of our experiments. We accounted for multiple testing by the Benjamini-Hochberg  
303 method with FDR=0.01 (61). Substitutions were biased toward C→T and G→A for all  
304 components in both experiments ( $p < 10^{-6}$ ). A bias toward C→A was observed in both  
305 experiments and toward G→T for all but ACMV DNA-B in the Veg6 experiment ( $p < 10^{-3}$ , see  
306 Table S3-4).

### 307 **Changes in viral diversity at the codon level**

308 To examine the impact of nucleotide diversity on amino acid codons, we looked at SNPs that  
309 passed our 3% threshold, occurred in both technical replicates, and were present in more than  
310 one passage (see Table S3-5 (Veg2) and S3-6 (Veg6) for a list of all of the SNPs found in at least  
311 two passages). ACMV had 125 codon changes, while EACMCV had 97 changes, with codon  
312 changes occurring in all ORFs of both viruses (Fig. 4a and b). When adjusted for ORF length,  
313 *ACI* of both viruses and ACMV *BVI* contained the fewest SNPs, with the other ORFs showing  
314 similar levels of SNPs (Fig. 4c and d). We also observed more non-synonymous SNPs than  
315 synonymous across both genomes (ACMV: N:80 S:49; EACMCV N:54 S:42). SIFT analysis  
316 predicted that the proportion of amino acid substitutions that negatively impact protein function  
317 was greater for EACMCV (65%) than for ACMV (52%, Table S3-6). Detrimental amino acid  
318 substitutions were predicted to occur in all viral ORFs. Some ORFs had higher number of non-  
319 synonymous mutations, with *AV2*, *AC4*, *AC5* of ACMV and *AC4* of EACMCV having the  
320 highest (Fig. 4a and b). When adjusted for ORF length, *ACI* and *BVI* had the lowest numbers  
321 and fraction of non-synonymous changes for both viruses. Rep is a complex enzyme that  
322 catalyzes multiple reactions necessary for viral replication (28) and, as such, may be less tolerant  
323 to amino acid substitution. In addition to viral DNA trafficking, NSP is engaged in a number of  
324 host interactions that may be sensitive to amino acid changes (40).

325

326 We asked how the SNPs impacted codons in known functional domains and motifs of the Rep  
327 protein (annotated in Fig. 1 and 2). The *ACI* ORFs of both viruses include long stretches devoid  
328 of polymorphisms, and the majority of changes were synonymous. ACMV *ACI* had synonymous  
329 SNPs in the DNA cleavage Motif 3 (62) and the Walker A helicase motif, while EACMCV *ACI*  
330 had a synonymous change in the Walker B helicase motif (63). The sequence of the EACMCV  
331 *AC2* promoter element that overlaps the Walker B motif was maintained in the mutant  
332 Tyr257Tyr (63). However, there were several non-synonymous changes distributed throughout  
333 the DNA binding/cleavage, oligomerization, and DNA helicase domains of their Rep proteins  
334 (29) (Table S3-6). Most notably, there was a SNP in EACMCV *ACI* that resulted in a Phe75Val  
335 codon change at a highly conserved position in the GRS motif (64).

336

337 We also looked at the potential effects of codon changes in other viral proteins. More SNPs were  
338 associated with ACMV *AC2* than EACMCV *AC2* (ACMV: 15, EACMCV: 5, Fig. 4). The amino  
339 acid changes were distributed across regions of the *AC2* protein associated with DNA binding  
340 (65), suppression of PTGS (66), and transcriptional activation (67). ACMV *AC3* was also  
341 associated with more SNPs than EACMCV *AC3* (ACMV: 16, EACMCV: 7, Fig. 4), and most of  
342 the SNPs in ACMV *AC3* resulted in non-synonymous codon changes, consistent with the  
343 capacity of REn to accommodate amino acid substitutions at many positions throughout the  
344 protein (68). The *AC3* gene contained the only codon change with a SNP in both viral genomes,  
345 i.e., Pro77 changing to Tyr in ACMV and to His in EACMCV. In contrast, the number of SNPs  
346 in *AVI* was similar for both viruses, with approximately half of the SNPs resulting in codon  
347 changes. The non-synonymous codon changes impacted amino acids associated with CP nuclear

348 localization, multimerization, and ssDNA binding (69), as well as whitefly transmission of  
349 begomoviruses (70-72). There were non-synonymous changes throughout the *BCI* gene of both  
350 viruses, some of which introduced amino acid changes at positions in the MP implicated in  
351 oligomerization (73) and subcellular targeting (74). One of the few non-synonymous codon  
352 changes in *BVI* was in the NSP nuclear export signal (75).

353

354 We also examined codon changes in regions where ORFs overlap on DNA-A. ACMV had more  
355 non-synonymous codon changes than synonymous ones in the region of *AVI* that overlaps with  
356 *AV2* and *AC5* (Fig. 4e and g), but no such bias was observed in the *AV2/AVI* overlapping region  
357 in EACMCV (Fig. 4f). Both viruses showed a tendency for non-synonymous changes to  
358 accumulate in the *AC4* ORF (Fig. 4e and f), which occurs entirely within *AC1*. Similar results  
359 have been reported for Tomato leaf deformation virus and Tomato yellow leaf curl virus (76,  
360 77). ACMV *AC2* and *AC3* both had a higher proportion of non-synonymous codon changes in  
361 their overlapping region (Fig. 4e), but this was not seen for EACMCV, which had non-  
362 synonymous codon changes in *AC3* but not *AC2* (Fig. 4f).

363

364 Some of the SNPs detected in the Veg6 experiment are also present in a historical database of  
365 CMB sequences available from GenBank (Table S3-7), as ascertained by querying recently  
366 described multiple alignments (Crespo et al., in preparation). Collectively, 19 Veg6 SNPs for  
367 ACMV DNA-A occurred 451 times in the set of 851 DNA-A sequences in GenBank  
368 (<http://zenodo.org/record/4029589>). Six EACMCV DNA-A Veg6 SNPs occurred 20 times in the  
369 same set of sequences, 3 ACMV DNA-B SNPs occurred 5 times (in a set of 104 sequences;  
370 <http://zenodo.org/record/3964979>), and 4 EACMCV DNA-B SNPs occurred one time each (in a

371 set of 243 sequences; <http://zenodo.org/record/3965023>) (78, 79). The SNPs represented in the  
372 historical database represent 9% of the total SNPs identified in the Veg6 study with 15%, 6%,  
373 8%, and 5% of the total SNPs identified for ACMV-A, ACMV-B, EACMCV-A, and EACMCV-  
374 B, respectively. This indicates that the majority of the SNPs observed in our studies are novel.  
375 The SNPs observed in our experiments, those currently in the historical database occurred at a  
376 higher allele frequency than those not represented in the historical database for ACMV-A at P 3-  
377 7, ACMV-B at P5-6, EACMV-A at P5 and P7, and EACMCV-B at P5 (P-value <0.05, Table S3-  
378 8). While we cannot rule out random genetic drift, these results beg further investigation of SNPs  
379 found in nature where, at certain passages may have been under positive selection in our  
380 experiments (Table S3-8). Yet, a majority of the changes found in the historical database for  
381 each genome segment were non-synonymous, except for in EACMCV-A where roughly equal  
382 numbers of synonymous and non-synonymous changes were observed (Table 3). Of the non-  
383 synonymous changes, 40% were predicted to be detrimental based on SIFT analysis (53) (Table  
384 S3-7).

385

### 386 **Changes in common region sequences**

387 We examined nucleotide changes that occurred during multiple passages in the noncoding  
388 sequences of DNA-A and DNA-B. There were 17 and 19 changes in the 5' intergenic sequences  
389 of ACMV DNA-A and DNA-B, respectively, while EACMCV had 12 and 35 changes in DNA-  
390 A and DNA-B, respectively (Table S3-6). We also observed 7 nucleotide changes in the 3'  
391 intergenic region of EACMCV-B, but none for the other viral components, which all have very  
392 short 3' intergenic regions with bidirectional polyadenylation signals (80).

393

394 The 5' intergenic regions of DNA-A and DNA-B contain a conserved sequence designated as the  
395 common region that contains the origin of replication and divergent promoter sequences (Fig. 5  
396 and 6). Changes in the common region occurred primarily outside of known conserved cis  
397 elements involved in replication (iterons and the stem loop (26, 27)) and transcription (TATA  
398 box, CLE element and CCAAT box (27, 81)). However, we observed an A→G change in the  
399 putative TATA box of the ACMV AV2 promoter (Table S3-6). We also detected G→C  
400 transversions in the stem sequences downstream of the nick site of both ACMV DNA-A and  
401 ACMV DNA-B (Fig. 5b), but we did not find compensatory changes in the upstream stem  
402 sequences. Given that the stem structure is necessary for viral replication (26), it was surprising  
403 that the 3'-stem SNPs were maintained in the population at a frequency of ca. 5% in at least 2  
404 passages of the Veg6 experiment. We observed a G→A transition at position 2626 in EACMCV-  
405 B. Comparison to the historical database indicated that the 5 G residues starting at position 2626  
406 constitute a third conserved iteron in the origin of replication (Fig. 6b; Table S3-7). However, the  
407 G at position 2626 is followed by 5 G residues, suggesting they can also serve as an origin iteron  
408 when G-2626 is mutated (82).

409

410 We also found that the common regions of the DNA-A components of both ACMV and  
411 EACMCV acquired mutations such that they more closely resembled the sequences of their  
412 cognate DNA-B common regions (Fig. 5b and 6b). This occurred in all bioreplicates of each  
413 passage in both Veg2 and Veg6 experiments. The ACMV DNA-A common region had SNPs at  
414 11 positions of which 9 matched ACMV-B (Fig. 5b). ACMV DNA-B had 5 SNPs, 3 at  
415 equivalent positions as ACMV-A substitutions. The EACMCV DNA-A common region had 5  
416 SNPs with 4 matching EACMCV DNA-B, and EACMCV DNA-B had 2 other SNPs (Fig. 6b).

417 We observed multiple deletions in the alignments of the ACMV DNA-A and EACMCV DNA-A  
418 common regions, while their cognate B components maintained the same length without indel  
419 mutations throughout all of the propagation experiments. There was a 7-bp deletion in EACMCV  
420 DNA-A in both the Veg2 and Veg6 experiments that resulted in a sequence match with  
421 EACMCV DNA-B, another mutation that made the DNA-A intergenic region better resemble  
422 that of the cognate DNA-B (Fig. 6b). The deletion was accompanied by CG→AA changes 11-12  
423 bp downstream. Mapping of the paired-end reads established that the 7-bp deletion and  
424 associated nucleotide changes in EACMCV DNA-A were not due to erroneous mapping of  
425 EACMCV DNA-B reads. Moreover, the deletion and nucleotide changes were not detected by  
426 Illumina sequencing of the plasmid controls, confirming that the variant was not present at low  
427 frequency in the EACMCV DNA-A inoculum. Together, these results suggested that the  
428 intergenic regions of ACMV DNA-A and EACMCV DNA-A sequences were less fit than those  
429 of their DNA-Bs, and there was selective pressure causing convergent evolution through inter-  
430 segment recombination with the more optimal sequences that resemble their cognate DNA-B  
431 sequences.

432

### 433 **Discussion**

434 Viruses exist as populations of related sequence variants (15). This reservoir of genetic diversity  
435 enables plant viral populations to change rapidly in response to environmental conditions,  
436 agricultural practices, and different hosts (17-20). Thus, understanding viral diversity and the  
437 external parameters that impact diversity is essential to develop durable disease resistance  
438 strategies. We characterized the genetic diversity of ACMV and EACMCV after inoculation of  
439 cassava plants with cloned viral sequences. We examined the effects of vegetative propagation as

440 an agriculture practice, temperature, and the presence of exogenous DNA sequences on the  
441 nucleotide diversity of the two CMBs. Our studies revealed that repeated vegetative propagation  
442 of infected cassava increased genome-wide nucleotide diversity of CMBs without detectable  
443 bottlenecks. Our experimental design starting from defined clones allowed us to confidently  
444 perform fine-scale analyses of genetic diversity using  $\pi$ , and to detect signatures of selection  
445 using Tajima's D involving large population sizes.

446

447 In our primary analysis of environmental factors, we found that vegetative propagation had the  
448 largest, and only significant, impact on CMB nucleotide diversity (Table 1 and 2). Multiple  
449 rounds of vegetative propagation of potato tubers infected with potato virus Y (PVY) also  
450 resulted in an overall increase in nucleotide diversity, and vegetative propagation had a larger  
451 effect on PVY diversity than vector transmission (83). Diversity profiles through passages varied  
452 depending on the PVY strain, with some strains increasing linearly and other strains peaking  
453 after the first vegetative passage and then decreasing (83). Our studies uncovered differences  
454 between CMB species, in that ACMV nucleotide diversity peaked at P4 and P6 and then  
455 decreased, while EACMCV diversity increased linearly through passages (Fig. 2 and Fig. S2a).  
456 Vegetative propagation was also the main factor leading to recombination events and generation  
457 of new geminivirus species in sweet potato (84, 85). Together, these results show how  
458 transmission mode impacts viral populations and evolution in root and tuber crops. Our results  
459 underscore the importance of discarding infected plants and providing access to virus-free  
460 planting material instead of using vegetative propagation to reduce virus spread and the  
461 emergence of new viral variants.

462



463 Surprisingly, increasing temperature had no significant impact on CMB nucleotide diversity  
464 (Supplementary Table 2). A 10°C shift has been associated with an increase in potexvirus  
465 nucleotide diversity in tomato, and the selection of SNPs in a strain-dependent manner (86). We  
466 used a 2°C temperature shift, based on predicted increases for global warming in Africa by 2030  
467 (47). The different outcomes in the two studies are likely due to the 5-fold difference in the  
468 temperature shifts but could also reflect differences in how DNA vs. RNA viruses or cassava vs.  
469 tomato plants respond to elevated temperatures. Nevertheless, our results suggest that the  
470 predicted 2°C temperature shift in Africa, may not be a main driver of CMB diversity (47).

471  
472 Some begomovirus satellites have been associated with elevated levels of viral DNA and  
473 suppression of host DNA methylation and silencing pathways (87), and as such have the  
474 potential to impact viral diversity. Although it is not known if SEGS-1 or SEGS-2 function in a  
475 similar manner, they have several features in common with satellites (46). We were unable to  
476 detect an effect of either SEGS-1 or SEGS-2 on viral nucleotide diversity in coinoculation  
477 experiments with CMBs (Table S3-1). However, these results do not rule out that other types of  
478 begomovirus satellites may impact viral diversity.

479  
480 We used Tajima's D to examine the patterns of nucleotide diversity through time and to gain  
481 insight into whether the CMB genomes were undergoing selection during vegetative  
482 propagation. Tajima's D compares the average number of pairwise differences with the number  
483 of segregating sites and determines selection or bottleneck pressure based on deviations from  
484 constant population size. Our analysis uncovered a significant positive change in variant  
485 frequency for both ACMV and EACMCV (Fig. 3), indicative of an increase in the number of

486 variants during vegetative propagation. However, the marginal significance is consistent with the  
487 generation of a population of intermediate variants from a founder event, i.e., inoculation of a  
488 cloned viral sequence, and that most variants are not under positive selection. The lack of  
489 selection pressure is consistent with the high level of variation in the amount of nucleotide  
490 diversity across passages (Fig. 2 and Fig. S2a). However, the intermediate variant population  
491 may undergo selection with more time, more passages, or most importantly, if the diverse  
492 population is exposed to a novel selection pressure. A similar phenomenon was observed for  
493 PVY SNP populations associated with 5 rounds of vegetative propagation of field-grown,  
494 infected potato (da Silva et al., 2020). These studies found that very few variants became fixed in  
495 the PVY population due to positive or negative selection, indicating that a small number of viral  
496 variants contributed to each new population after propagation (83). In our study, the variation in  
497 nucleotide diversity patterns across the CMB genomic components from one passage to the next  
498 (Fig. S2a) is consistent with a small fraction of viral variants propagated to the next generation  
499 with no mutations fixed in the population for more than 3 passages.

500

501 We observed more non-synonymous changes than synonymous changes in the genomes of both  
502 ACMV and EACMCV (Fig. 4c and d), which is consistent with the higher possibility of non-  
503 synonymous mutations in coding regions by random chance. However, a large fraction of the  
504 non-synonymous codon changes also observed in both viruses were predicted to cause  
505 detrimental amino acid substitutions using SIFT analysis, which has been correlated with a lack  
506 of purifying selection (88). The strongest effects of purifying selection (fewest non-synonymous  
507 changes, large stretches without changes) was observed in AC1, not AVI as has been observed in  
508 field isolates of EACMV (10). This difference is likely a direct result of the vegetative

509 transmission mode being tested here; many plant viruses have strong purifying selection on their  
510 capsid proteins because of their interactions with both plant and insects (89). During vegetative  
511 propagation of CMVs there is no selective pressure from a whitefly vector, and we see that  
512 relaxation in the higher numbers of non-synonymous changes in *AVI* compared to *ACI*. While  
513 these results rule out strong purifying selection acting on CMB viral ORFs, we cannot rule out  
514 balancing selection within the timeframe of our studies based on the results of Tajima's D. The  
515 presence of SNPs from our experiment in field-collected sequences in GenBank means that some  
516 of the variation we observe is not so deleterious as to never be isolated in nature, but we saw no  
517 evidence that this subset of SNPs was under more positive selection in our vegetative passaging.  
518 Because field populations of CMBs are not exhaustively sequenced, it remains unclear what  
519 fraction of the SNPs in this experiment have and would persist and thrive in the field.

520

521 Unlike the viral ORFs, we observed multiple nucleotide substitutions in the common regions of  
522 the A components of ACMV and EACMCV that were present in all bioreplicates, resulting in  
523 sequences that more closely resembled the common regions of their cognate B components. The  
524 common region includes cis-acting sequences that are necessary for replication. When an  
525 infectious clone is made, a single sequence is cloned out of the viral population in the source  
526 plant, and that sequence must have a functional origin to be viable infectious clone. This is in  
527 stark contrast to viral sequences carrying detrimental codon mutations, which can be  
528 complemented in trans by other viral components carrying functional promoters and ORFs (90).  
529 However, the cloned sequence may not have an efficient origin and, thus, would be under  
530 selective pressure to better compete with more efficient origin sequences. This type of  
531 competition was seen in origin mutants of Tomato golden mosaic virus (TGMV) DNA-B in

532 protoplast replication assays (26). Hence, the convergence of CMB DNA-A common region  
533 sequences toward DNA-B may reflect evolutionary selection of a more efficient origin through  
534 sequentially acquired intersegment recombination, which would explain the multiple similar  
535 substitutions more easily than sequential acquisition of independent mutations. Examples of  
536 intersegment (inter-component) recombination of common regions have been observed during  
537 passaging in *Nicotiana benthamiana* plants under laboratory conditions with tomato mottle virus,  
538 bean dwarf mosaic virus, and African cassava mosaic virus (91, 92), but the directionality has  
539 previously always been a DNA-B common region becoming more like DNA-A. Intersegment  
540 recombination of the common region has also been frequently observed in the ssDNA  
541 phytopathogenic nanoviruses, which have six or more genome components (93).

542

543 Nucleotide substitution bias has been observed for geminivirus sequences in historical datasets  
544 (10) and in experimental populations examined within single plants infected for up to five years  
545 (94, 95). Our results showed that nucleotide substitution biases are readily detected in a 2-month  
546 timeframe for ACMV and EACMCV, and that this short time is sufficient to detect nucleotide  
547 substitution biases in both transitions (C→T and G→A), consistent with historical sequences of  
548 East African cassava mosaic virus (10) and experimental infection of Tomato yellow leaf curl  
549 China virus (95) and one transversion (G→T, previously reported for experimental populations  
550 (94)) for both viruses. It has been proposed that the nucleotide substitution bias is due to  
551 oxidative damage (10, 94). The repeated pattern of nucleotide substitution bias in our  
552 experiments points to oxidative damage (96). The C→T and G→A transitions could be due to  
553 hydroxylation mediated by reactive oxygen species, possibly by oxidative deamination of  
554 cytosine in the case of C→T mutations (97), and the G→T transversions could be from oxidative

555 damage converting guanine to 8-oxoguanine, which base pairs with adenine leading to a G-C  
556 base pair mutating to a T-A base pair (98). Our SNP nucleotide biases match the substitution  
557 biases of ssDNA virus historical data sets, showing that the same molecular patterns can be  
558 observed over months as decades.

559

560 This study provides evidence that farming practices, such as vegetative propagation, can have a  
561 large impact on genetic diversity across CMB genome components. This study also presents  
562 evidence that CMB genes are under relaxed selection pressure during vegetative propagation,  
563 with *ACI* and *BVI* under the strongest purifying selection pressure. This is not the case for the  
564 intergenic region, especially in the convergence of the DNA-A common region sequences  
565 toward DNA-B, likely reflecting selection of a more efficient origin. This pattern is consistent  
566 with mutated viral genomes being able to complement protein functions in trans, but there being  
567 strong selection for optimal origin of replication function, which cannot be complemented.  
568 Understanding how CMBs and other ssDNA viruses are evolving through experimental  
569 evolution studies such as this will ultimately help inform and improve strategies for disease  
570 management.

571

### 572 **Funding information**

573 This work was supported by the National Science Foundation grant OISE-1545553 to L.H.-B,  
574 G.G.K., and S.D. CDA was supported with NSF Graduate Research Fellowship and an NCSU  
575 Provost Fellowship. LDLG was supported by a Fulbright Fellowship.

576

### 577 **Acknowledgments**

578 We thank Mary Beth Dallas for her help growing cassava plants. Infectious clones were  
579 generously provided by Vincent Fondong (Addgene plasmids 159134 to 159137;  
580 <https://www.addgene.org/browse/article/28211870/>). We thank the NC State University Genome  
581 Science Laboratory for their support. The Cassava Virus Evolution Galaxy server  
582 (<https://cassavavirusevolution.vcl.ncsu.edu/>) is hosted in the NC State University Virtual  
583 Computing Lab, and we thank Matthew Gronke, Saahil Chawande, and Jim White for server  
584 setup and maintenance. This work also used the Amarel cluster maintained by the Office of  
585 Advanced Research Computing (OARC) at Rutgers, The State University of New Jersey.

586

#### 587 **Author contributions**

588 C.A. and E.L. were responsible for writing and preparing the manuscript, experimental design,  
589 collection, and data analysis. J.S.H. was responsible for experimental design and data analysis.  
590 D.D. and L.M.-Y. conducted library preparation. L.H.-B., S.D., A.L.J, I.C., and G.G.K. were  
591 responsible for experimental design and manuscript preparation.

592

#### 593 **Conflicts of interest**

594 The authors declare that there are no conflicts of interest.

595

#### 596 **References**

- 597 1. Rojas MR, Macedo MA, Maliano MR, Soto-Aguilar M, Souza JO, Briddon RW, et al. World  
598 Management of Geminiviruses. *Annual review of phytopathology*. 2018;56(1):637-77.  
599 2. Hanley-Bowdoin L, Bejarano ER, Robertson D, Mansoor S. Geminiviruses: masters at  
600 redirecting and reprogramming plant processes. *Nature reviews Microbiology*. 2013;11(11):777-88.  
601 3. Kumar RV. Plant Antiviral Immunity Against Geminiviruses and Viral Counter-Defense for  
602 Survival. *Front Microbiol*. 2019;10.  
603 4. Denhardt DT, Silver RB. An analysis of the clone size distribution of phi-X-174 mutants and  
604 recombinants. *Virology*. 1966;30(1):10-9.

- 605 5. Fersht AR. Fidelity of replication of phage phi X174 DNA by DNA polymerase III holoenzyme:  
606 spontaneous mutation by misincorporation. *Proc Natl Acad Sci U S A.* 1979;76(10):4946-50.
- 607 6. Raney JL, Delongchamp RR, Valentine CR. Spontaneous mutant frequency and mutation  
608 spectrum for gene A of phiX174 grown in *E. coli*. *Environmental and molecular mutagenesis.*  
609 2004;44(2):119-27.
- 610 7. Shackelton LA, Parrish CR, Truyen U, Holmes EC. High rate of viral evolution associated with  
611 the emergence of carnivore parvovirus. *Proc Natl Acad Sci U S A.* 2005;102(2):379-84.
- 612 8. Firth C, Charleston MA, Duffy S, Shapiro B, Holmes EC. Insights into the evolutionary history  
613 of an emerging livestock pathogen: porcine circovirus 2. *Journal of virology.* 2009;83(24):12813-21.
- 614 9. Grigoras I, Timchenko T, Grande-Pérez A, Katul L, Vetten H-J, Gronenborn B. High Variability  
615 and Rapid Evolution of a Nanovirus. *Journal of virology.* 2010;84(18):9105-17.
- 616 10. Duffy S, Holmes EC. Validation of high rates of nucleotide substitution in geminiviruses:  
617 phylogenetic evidence from East African cassava mosaic viruses. *The Journal of general virology.*  
618 2009;90(Pt 6):1539-47.
- 619 11. Rocha CS, Castillo-Urquiza GP, Lima ATM, Silva FN, Xavier CAD, Hora-Júnior BT, et al.  
620 Brazilian Begomovirus Populations Are Highly Recombinant, Rapidly Evolving, and Segregated Based  
621 on Geographical Location. *Journal of virology.* 2013;87(10):5784-99.
- 622 12. Pita JS, Fondong VN, Sangaré A, Otim-Nape GW, Ogwal S, Fauquet CM. Recombination,  
623 pseudorecombination and synergism of geminiviruses are determinant keys to the epidemic of severe  
624 cassava mosaic disease in Uganda. *The Journal of general virology.* 2001;82(Pt 3):655-65.
- 625 13. Lima ATM, Silva JCF, Silva FN, Castillo-Urquiza GP, Silva FF, Seah YM, et al. The  
626 diversification of begomovirus populations is predominantly driven by mutational dynamics. *Virus*  
627 *evolution.* 2017;3(1):vex005.
- 628 14. Lefeuve P, Moriones E. Recombination as a motor of host switches and virus emergence:  
629 geminiviruses as case studies. *Current Opinion in Virology.* 2015;10:14-9.
- 630 15. Elena SF, Sanjuán R. Virus Evolution: Insights from an Experimental Approach. *Annual Review*  
631 *of Ecology, Evolution, and Systematics.* 2007;38(1):27-52.
- 632 16. Safari M, Roossinck MJ. How does the genome structure and lifestyle of a virus affect its  
633 population variation? *Current Opinion in Virology.* 2014;9:39-44.
- 634 17. DeFilippis VR, Villarreal LP. An Introduction to the Evolutionary Ecology of Viruses. *Viral*  
635 *Ecology.* 2000:125-208.
- 636 18. Bernardo P, Charles-Dominique T, Barakat M, Ortet P, Fernandez E, Filloux D, et al.  
637 Geometagenomics illuminates the impact of agriculture on the distribution and prevalence of plant viruses  
638 at the ecosystem scale. *The ISME Journal.* 2018;12(1):173-84.
- 639 19. Bergès SE, Vile D, Vazquez-Rovere C, Blanc S, Yvon M, Bédiée A, et al. Interactions Between  
640 Drought and Plant Genotype Change Epidemiological Traits of Cauliflower mosaic virus. *Front Plant Sci.*  
641 2018;9:703-.
- 642 20. Roberts KE, Hadfield JD, Sharma MD, Longdon B. Changes in temperature alter the potential  
643 outcomes of virus host shifts. *PLoS Pathog.* 2018;14(10):e1007185-e.
- 644 21. FAOSTAT. FAO Statistical Databases. <http://faostatfaorg/>. 2016;Food and Agriculture  
645 Organization (FAO) of the United Nations, Rome, Italy
- 646 22. Legg JP, Lava Kumar P, Makesh Kumar T, Tripathi L, Ferguson M, Kanju E, et al. Cassava virus  
647 diseases: biology, epidemiology, and management. *Advances in virus research.* 2015;91:85-142.
- 648 23. Stanley J, Gay MR. Nucleotide sequence of of cassava latent virus DNA. *Nature.* 1983;301:2660-  
649 2.
- 650 24. Sanjuán R. From Molecular Genetics to Phylodynamics: Evolutionary Relevance of Mutation  
651 Rates Across Viruses. *PLoS Pathog.* 2012;8(5):e1002685.
- 652 25. Hicks AL, Duffy S. Cell Tropism Predicts Long-term Nucleotide Substitution Rates of  
653 Mammalian RNA Viruses. *PLoS Pathog.* 2014;10(1):e1003838.
- 654 26. Orozco BM, Hanley-Bowdoin L. A DNA structure is required for geminivirus replication origin  
655 function. *Journal of virology.* 1996;70 1:148-58.



- 656 27. Argüello-Astorga GR, Guevara-González RG, Herrera-Estrella LR, Rivera-Bustamante RF.  
657 Geminivirus replication origins have a group-specific organization of iterative elements: a model for  
658 replication. *Virology*. 1994;203(1):90-100.
- 659 28. Laufs J, Traut W, Heyraud F, Matzeit V, Rogers SG, Schell J, et al. In vitro cleavage and joining  
660 at the viral origin of replication by the replication initiator protein of tomato yellow leaf curl virus.  
661 *Proceedings of the National Academy of Sciences of the United States of America*. 1995;92(9):3879-83.
- 662 29. Clérot D, Bernardi F. DNA helicase activity is associated with the replication initiator protein rep  
663 of tomato yellow leaf curl geminivirus. *Journal of virology*. 2006;80(22):11322-30.
- 664 30. Elmer JS, Brand L, Sunter G, Gardiner WE, Bisaro DM, Rogers SG. Genetic analysis of the  
665 tomato golden mosaic virus. II. The product of the AL1 coding sequence is required for replication.  
666 *Nucleic acids research*. 1988;16(14b):7043-60.
- 667 31. Wu M, Wei H, Tan H, Pan S, Liu Q, Bejarano ER, et al. Plant DNA polymerases alpha and delta  
668 mediate replication of geminiviruses. *bioRxiv*. 2020:2020.07.20.212167.
- 669 32. Jeske H, Lütgemeier M, Preiß W. DNA forms indicate rolling circle and  
670 recombination-independent replication of Abutilon mosaic virus. *The EMBO Journal*. 2001;20(21):6158-  
671 67.
- 672 33. Hipp K, Grimm C, Jeske H, Böttcher B. Near-Atomic Resolution Structure of a Plant  
673 Geminivirus Determined by Electron Cryomicroscopy. *Structure*. 2017;25(8):1303-9.e3.
- 674 34. Sunter G, Bisaro DM. Transactivation of geminivirus AR1 and BR1 gene expression by the viral  
675 AL2 gene product occurs at the level of transcription. *The Plant Cell*. 1992;4(10):1321.
- 676 35. Loriato VAP, Martins LGC, Euclides NC, Reis PAB, Duarte CEM, Fontes EPB. Engineering  
677 resistance against geminiviruses: A review of suppressed natural defenses and the use of RNAi and the  
678 CRISPR/Cas system. *Plant science : an international journal of experimental plant biology*.  
679 2020;292:110410.
- 680 36. Li F, Xu X, Huang C, Gu Z, Cao L, Hu T, et al. The AC5 protein encoded by Mungbean yellow  
681 mosaic India virus is a pathogenicity determinant that suppresses RNA silencing-based antiviral defenses.  
682 *The New phytologist*. 2015;208(2):555-69.
- 683 37. Stanley J, Gay MR. Nucleotide sequence of cassava latent virus DNA. *Nature*.  
684 1983;301(5897):260-2.
- 685 38. Noueiry AO, Lucas WJ, Gilbertson RL. Two proteins of a plant DNA virus coordinate nuclear  
686 and plasmodesmal transport. *Cell*. 1994;76(5):925-32.
- 687 39. Sanderfoot AA, Lazarowitz SG. Cooperation in Viral Movement: The Geminivirus BL1  
688 Movement Protein Interacts with BR1 and Redirects It from the Nucleus to the Cell Periphery. *The Plant*  
689 *Cell*. 1995;7(8):1185.
- 690 40. Martins LGC, Raimundo GAS, Ribeiro NGA, Silva JCF, Euclides NC, Loriato VAP, et al. A  
691 Begomovirus Nuclear Shuttle Protein-Interacting Immune Hub: Hijacking Host Transport Activities and  
692 Suppressing Incompatible Functions. *Front Plant Sci*. 2020;11(398).
- 693 41. Fondong VN, Pita JS, Rey MEC, de Kochko A, Beachy RN, Fauquet CM. Evidence of synergism  
694 between African cassava mosaic virus and a new double-recombinant geminivirus infecting cassava in  
695 Cameroon. *Journal of General Virology*. 2000;81(1):287-97.
- 696 42. Deng D, Otim-Nape WG, Sangare A, Ogwal S, Beachy RN, Fauquet CM. Presence of a new  
697 virus closely related to East African cassava mosaic geminivirus, associated with cassava mosaic outbreak  
698 in Uganda. *African J Root Tuber Crops*. 1997;2:23-8.
- 699 43. Rabbi IY, Hamblin MT, Kumar PL, Gedil MA, Ikpan AS, Jannink J-L, et al. High-resolution  
700 mapping of resistance to cassava mosaic geminiviruses in cassava using genotyping-by-sequencing and  
701 its implications for breeding. *Virus Research*. 2014;186:87-96.
- 702 44. Akano A, Dixon A, Mba C, Barrera E, Fregene M. Genetic mapping of a dominant gene  
703 conferring resistance to cassava mosaic disease. *Theoretical and Applied Genetics*. 2002;105(4):521-5.
- 704 45. Ndunguru J, De Leon L, Doyle CD, Sseruwagi P, Plata G, Legg JP, et al. Two Novel DNAs That  
705 Enhance Symptoms and Overcome CMD2 Resistance to Cassava Mosaic Disease. *Journal of virology*.  
706 2016;90(8):4160-73.



- 707 46. Aimone CD, De Leon L, Dallas MM, Ndunguru J, Ascencio-Ibanez JT, Hanley-Bowdoin L. A  
708 New Type of Satellite associated with Cassava Mosaic Begomoviruses. bioRxiv.  
709 2021:2021.03.11.434950.
- 710 47. Jarvis A, Ramirez-Villegas J, Campo BVH, Navarro-Racines C. Is cassava the answer to African  
711 climate change adaptation? *Trop Plant Biol.* 2012;5:9–29.
- 712 48. Hoyer JS, Fondong VN, Dallas MM, Aimone CD, Deppong DO, Duffy S, et al. Deeply  
713 Sequenced Infectious Clones of Key Cassava Begomovirus Isolates from Cameroon. *Microbiology  
714 Resource Announcements.* 2020;9(46):e00802-20.
- 715 49. Fondong VN, Chen K. Genetic variability of East African cassava mosaic Cameroon virus under  
716 field and controlled environment conditions. *Virology.* 2011;413(2):275-82.
- 717 50. Aimone CD, Hoyer JS, Dye AE, Deppong DO, Duffy S, Carbone I, et al. An improved  
718 experimental pipeline for preparing circular ssDNA viruses for next-generation sequencing. bioRxiv.  
719 2020:2020.09.30.321224.
- 720 51. Koboldt DC, Zhang Q, Larson DE, Shen D, McLellan MD, Lin L, et al. VarScan 2: somatic  
721 mutation and copy number alteration discovery in cancer by exome sequencing. *Genome research.*  
722 2012;22(3):568-76.
- 723 52. Cingolani P, Platts A, Wang le L, Coon M, Nguyen T, Wang L, et al. A program for annotating  
724 and predicting the effects of single nucleotide polymorphisms, SnpEff: SNPs in the genome of *Drosophila  
725 melanogaster* strain w1118; iso-2; iso-3. *Fly.* 2012;6(2):80-92.
- 726 53. Kumar P, Henikoff S, Ng PC. Predicting the effects of coding non-synonymous variants on  
727 protein function using the SIFT algorithm. *Nature Protocols.* 2009;4(7):1073-81.
- 728 54. Smith TF, Waterman MS. Identification of common molecular subsequences. *Journal of  
729 molecular biology.* 1981;147(1):195-7.
- 730 55. Nei M, Li WH. Mathematical model for studying genetic variation in terms of restriction  
731 endonucleases. *Proceedings of the National Academy of Sciences.* 1979;76(10):5269-73.
- 732 56. Kofler R, Pandey RV, Schlötterer C. PoPoolation2: identifying differentiation between  
733 populations using sequencing of pooled DNA samples (Pool-Seq). *Bioinformatics.* 2011;27(24):3435-6.
- 734 57. Seabold S, and Josef Perktold. statsmodels: Econometric and statistical modeling with python.  
735 *Proceedings of the 9th Python in Science Conference.* 2010.
- 736 58. Peck DCMAEA. *Introduction to Linear Regression Analysis.* 2nd ed: Wiley; 1992.
- 737 59. Tajima F. Statistical method for testing the neutral mutation hypothesis by DNA polymorphism.  
738 *Genetics.* 1989;123(3):585-95.
- 739 60. Harkins GW, Delpont W, Duffy S, Wood N, Monjane AL, Owor BE, et al. Experimental evidence  
740 indicating that mastreviruses probably did not co-diverge with their hosts. *Virology Journal.*  
741 2009;6(1):104.
- 742 61. Benjamini Y, Hochberg Y. Controlling the False Discovery Rate: A Practical and Powerful  
743 Approach to Multiple Testing. *Journal of the Royal Statistical Society: Series B (Methodological).*  
744 1995;57(1):289-300.
- 745 62. Orozco BM, Hanley-Bowdoin L. Conserved sequence and structural motifs contribute to the  
746 DNA binding and cleavage activities of a geminivirus replication protein. *The Journal of biological  
747 chemistry.* 1998;273(38):24448-56.
- 748 63. George B, Ruhel R, Mazumder M, Sharma VK, Jain SK, Gourinath S, et al. Mutational analysis  
749 of the helicase domain of a replication initiator protein reveals critical roles of Lys 272 of the B' motif and  
750 Lys 289 of the  $\beta$ -hairpin loop in geminivirus replication. *The Journal of general virology.* 2014;95(Pt  
751 7):1591-602.
- 752 64. Nash TE, Dallas MB, Reyes MI, Buhrman GK, Ascencio-Ibañez JT, Hanley-Bowdoin L.  
753 Functional analysis of a novel motif conserved across geminivirus Rep proteins. *Journal of virology.*  
754 2011;85(3):1182-92.
- 755 65. Sung YK, Coutts RH. Potato yellow mosaic geminivirus AC2 protein is a sequence non-specific  
756 DNA binding protein. *FEBS Lett.* 1996;383(1-2):51-4.

- 757 66. Trinks D, Rajeswaran R, Shivaprasad PV, Akbergenov R, Oakeley EJ, Veluthambi K, et al.  
758 Suppression of RNA silencing by a geminivirus nuclear protein, AC2, correlates with transactivation of  
759 host genes. *Journal of virology*. 2005;79(4):2517-27.
- 760 67. Wang H, Buckley KJ, Yang X, Buchmann RC, Bisaro DM. Adenosine kinase inhibition and  
761 suppression of RNA silencing by geminivirus AL2 and L2 proteins. *Journal of virology*.  
762 2005;79(12):7410-8.
- 763 68. Settlage SB, See RG, Hanley-Bowdoin L. Geminivirus C3 protein: replication enhancement and  
764 protein interactions. *Journal of virology*. 2005;79(15):9885-95.
- 765 69. Qin S, Ward BM, Lazarowitz SG. The Bipartite Geminivirus Coat Protein Aids BR1 Function in  
766 Viral Movement by Affecting the Accumulation of Viral Single-Stranded DNA. *Journal of virology*.  
767 1998;72(11):9247.
- 768 70. Kheyr-Pour A, Bananej K, Dafalla GA, Caciagli P, Noris E, Ahoonmanesh A, et al. Watermelon  
769 chlorotic stunt virus from the Sudan and Iran: Sequence Comparisons and Identification of a Whitefly-  
770 Transmission Determinant. *Phytopathology*. 2000;90(6):629-35.
- 771 71. Caciagli P, Medina Piles V, Marian D, Vecchiati M, Masenga V, Mason G, et al. Virion Stability  
772 Is Important for the Circulative Transmission of *Tomato Yellow Leaf Curl Sardinia Virus* by  
773 *Bemisia tabaci*, but Virion Access to Salivary Glands Does Not Guarantee Transmissibility.  
774 *Journal of virology*. 2009;83(11):5784-95.
- 775 72. Höhnle M, Höfer P, Bedford ID, Briddon RW, Markham PG, Frischmuth T. Exchange of three  
776 amino acids in the coat protein results in efficient whitefly transmission of a nontransmissible Abutilon  
777 mosaic virus isolate. *Virology*. 2001;290(1):164-71.
- 778 73. Kleinow T, Nischang M, Beck A, Kratzer U, Tanwir F, Preiss W, et al. Three C-terminal  
779 phosphorylation sites in the Abutilon mosaic virus movement protein affect symptom development and  
780 viral DNA accumulation. *Virology*. 2009;390(1):89-101.
- 781 74. Zhang SC, Ghosh R, Jeske H. Subcellular targeting domains of Abutilon mosaic geminivirus  
782 movement protein BC1. *Archives of Virology*. 2002;147(12):2349-63.
- 783 75. Ward BM, Lazarowitz SG. Nuclear Export in Plants: Use of Geminivirus Movement Proteins for  
784 a Cell-Based Export Assay. *The Plant Cell*. 1999;11(7):1267-76.
- 785 76. Melgarejo TA, Kon T, Rojas MR, Paz-Carrasco L, Zerbini FM, Gilbertson RL. Characterization  
786 of a new world monopartite begomovirus causing leaf curl disease of tomato in Ecuador and Peru reveals  
787 a new direction in geminivirus evolution. *Journal of virology*. 2013;87(10):5397-413.
- 788 77. Yang X-l, Zhou M-n, Qian Y-j, Xie Y, Zhou X-p. Molecular variability and evolution of a natural  
789 population of tomato yellow leaf curl virus in Shanghai, China. *Journal of Zhejiang University SCIENCE*  
790 *B*. 2014;15(2):133-42.
- 791 78. Dubey D, Hoyer, J. Steen, & Duffy, Siobain. Multiple alignment of ACMV and ACMBFV DNA-  
792 B sequences Zenodo2020.
- 793 79. Crespo-Bellido A, & Duffy, Siobain. Multiple sequence alignment of DNA-A sequences from  
794 ACMBFV, ACMV, CMMGV, EACMCV, EACMKV, EACMMV, EACMV, EACMZV, SACMV,  
795 ICMV, SLCMV (11 species) Zenodo2020.
- 796 80. Hanley-Bowdoin L, Settlage SB, Orozco BM, Nagar S, Robertson D. Geminiviruses: Models for  
797 Plant DNA Replication, Transcription, and Cell Cycle Regulation. *Critical Reviews in Plant Sciences*.  
798 1999;18(1):71-106.
- 799 81. Cantú-Iris M, Pastor-Palacios G, Mauricio-Castillo JA, Bañuelos-Hernández B, Avalos-Calleros  
800 JA, Juárez-Reyes A, et al. Analysis of a new begomovirus unveils a composite element conserved in the  
801 CP gene promoters of several Geminiviridae genera: Clues to comprehend the complex regulation of late  
802 genes. *PloS one*. 2019;14(1):e0210485.
- 803 82. Argüello-Astorga GR, Ruiz-Medrano R. An iteron-related domain is associated to Motif 1 in the  
804 replication proteins of geminiviruses: identification of potential interacting amino acid-base pairs by a  
805 comparative approach. *Archives of Virology*. 2001;146(8):1465-85.
- 806 83. da Silva W, Kutnjak D, Xu Y, Xu Y, Giovannoni J, Elena SF, et al. Transmission modes affect  
807 the population structure of potato virus Y in potato. *PLoS Pathog*. 2020;16(6):e1008608.

- 808 84. Paprotka T, Boiteux LS, Fonseca MEN, Resende RO, Jeske H, Faria JC, et al. Genomic diversity  
809 of sweet potato geminiviruses in a Brazilian germplasm bank. *Virus Research*. 2010;149(2):224-33.
- 810 85. Nhlapo TF, Rees DJG, Odeny DA, Mulabisana JM, Rey MEC. Viral metagenomics reveals sweet  
811 potato virus diversity in the Eastern and Western Cape provinces of South Africa. *South African Journal*  
812 *of Botany*. 2018;117:256-67.
- 813 86. Alcaide C, Sardanyés J, Elena SF, Gómez P. Increasing growth temperature alters the within-host  
814 competition of viral strains and influences virus genetic variation. *bioRxiv*. 2020:2020.07.06.190173.
- 815 87. Nawaz-ul-Rehman MS, Fauquet CM. Evolution of geminiviruses and their satellites. *FEBS Lett*.  
816 2009;583(12):1825-32.
- 817 88. Yang Z, Bielawski JP. Statistical methods for detecting molecular adaptation. *Trends in Ecology*  
818 *& Evolution*. 2000;15(12):496-503.
- 819 89. Chare ER, Holmes EC. Selection pressures in the capsid genes of plant RNA viruses reflect mode  
820 of transmission. *The Journal of general virology*. 2004;85(Pt 10):3149-57.
- 821 90. Fondong VN. Geminivirus protein structure and function. *Molecular Plant Pathology*.  
822 2013;14(6):635-49.
- 823 91. Roberts S, Stanley J. Lethal mutations within the conserved stem-loop of African cassava mosaic  
824 virus DNA are rapidly corrected by genomic recombination. *The Journal of general virology*. 1994;75 ( Pt  
825 11):3203-9.
- 826 92. Hou YM, Gilbertson RL. Increased pathogenicity in a pseudorecombinant bipartite geminivirus  
827 correlates with intermolecular recombination. *Journal of virology*. 1996;70(8):5430-6.
- 828 93. Martin DP, Biagini P, Lefeuvre P, Golden M, Roumagnac P, Varsani A. Recombination in  
829 eukaryotic single stranded DNA viruses. *Viruses*. 2011;3(9):1699-738.
- 830 94. van der Walt E, Martin DP, Varsani A, Polston JE, Rybicki EP. Experimental observations of  
831 rapid Maize streak virus evolution reveal a strand-specific nucleotide substitution bias. *Virology Journal*.  
832 2008;5(1):104.
- 833 95. Ge L, Zhang J, Zhou X, Li H. Genetic Structure and Population Variability of Tomato Yellow  
834 Leaf Curl China Virus. *Journal of virology*. 2007;81(11):5902-7.
- 835 96. Frederico LA, Kunkel TA, Shaw BR. A sensitive genetic assay for the detection of cytosine  
836 deamination: determination of rate constants and the activation energy. *Biochemistry*. 1990;29(10):2532-  
837 7.
- 838 97. Kreutzer DA, Essigmann JM. Oxidized, deaminated cytosines are a source of C --> T transitions  
839 in vivo. *Proc Natl Acad Sci U S A*. 1998;95(7):3578-82.
- 840 98. David SS, O'Shea VL, Kundu S. Base-excision repair of oxidative DNA damage. *Nature*.  
841 2007;447(7147):941-50.
- 842 99. Koonin EV, Ilyina TV. Geminivirus replication proteins are related to prokaryotic plasmid rolling  
843 circle DNA replication initiator proteins. *Journal of General Virology*. 1992;73(10):2763-6.

844

845

846 **TABLES AND FIGURE LEGENDS**

847 **Table 1.** Veg2, ANOVA results of nucleotide diversity as a response to experimental variables.

848 Model  $R^2 = 0.834$ . Model  $p = 0.00115$ .

849

	Degrees of Freedom	Sum of Squares	Mean Square	F	p
<b>Species</b>	1	7.78	7.78	0.395	0.5496
<b>Species: Segment</b>	2	27.45	13.73	0.697	0.5296
<b>Passage</b>	1	658.75	658.75	33.453	<i>0.0007</i>
<b>Residual</b>	7	137.84	19.69		

850

851 **Table 2.** Veg6, ANOVA results of nucleotide diversity as a response to experimental variables.

852 Model  $R^2 = 0.438$ . Model  $p = 0.00537$

853

	Degrees of Freedom	Sum of Squares	Mean Square	F	p
<b>Species</b>	1	231.4	231.4	2.06	0.165
<b>Species: Segment</b>	2	149.2	74.6	0.66	0.525
<b>Passage</b>	1	1632.6	1632.6	14.51	<i>0.0009</i>
<b>Residual</b>	23	2587.0	112.5		

854

855 **Table 3.** Number of SNPs observed in the historical database for Veg6 experiment by genome

856 component.

	ACMV-A	ACMV-B	EACMCV-A	EACMCV-B
Synonymous	5	1	3	0
Non-Synonymous	14	2	3	4

857

858 **Fig 1. ACMV and EACMCV nucleotide diversity in the Veg2 experiment.** (a) Sliding  
859 window analysis of nucleotide diversity ( $\pi$ ) of ACMV DNA-A and DNA-B and (c) EACMCV  
860 DNA-A and DNA-B. Dark pink to lighter pink represents the nucleotide diversity across the  
861 genome of inoculated plants (P1) and two vegetative propagations (P2 and P3). Enhanced views  
862 of the nucleotide diversity of the *AVI* and *ACI* open reading frames during P1-P3 for ACMV-A  
863 (b) and EACMCV-A (d). Blue lines mark the locations of codons encoding functional motifs in  
864 the Rep protein, i.e. Rep C, Rep B, Walker B, Walker A (63), Motif 3 (62), GRS (64), Motif 2  
865 (62) and Motif 1 (82). The motifs are shown to scale. Genome coordinates (nt), the positions of  
866 open reading frames and their directions of transcription are shown below each graph.

867 **Fig 2. Veg6 ACMV and EACMCV nucleotide diversity sliding windows.** (a) Sliding window  
868 analysis of nucleotide diversity ( $\pi$ ) of ACMV DNA-A and DNA-B and (c) EACMCV DNA-A  
869 and DNA-B. Dark pink to dark green represents the nucleotide diversity across the genome of  
870 inoculated plants (P1) and two vegetative propagations (P4 and P6). Enhanced views of the  
871 nucleotide diversity of the *AVI* and *ACI* open reading frames during P1, P4, and P7 for ACMV-  
872 A (b) and EACMCV-A (d). Blue lines mark the locations of codons encoding functional motifs  
873 in the Rep protein, i.e. Rep C, Rep B, Walker B, Walker A (63), Motif 3 (62), GRS (64), Motif 2  
874 (62) and Motif 1 (82). The motifs are shown to scale. Genome coordinates (nt), the positions of  
875 open reading frames and their directions of transcription are shown below each graph.

876 **Fig 3. Tajima's D analysis by passage and minimum variant frequency cutoff.** Tajima's D  
877 analysis passage (P) for (a) ACMV DNA-A and DNA-B and (b) EACMCV DNA-A and DNA-B  
878 in the Veg2 experiment. Tajima's D by passage for (c) ACMV DNA-A and DNA-B and (d)  
879 EACMCV DNA-A and DNA-B in the Veg6 experiment. Dotted red horizontal lines represent  
880 thresholds for significant Tajima's D values (59). The vertical blue dotted line represents the

881 minimum variant frequency of 3% used in this study. The lines representing each passage are  
882 color coded, as shown at the bottom.

883 **Fig 4. Synonymous and non-synonymous codon changes in ACMV and EACMCV.**

884 Diagram of the locations of synonymous codon changes (grey), unassigned changes in  
885 overlapping open reading frames (ORFs; green), and non-synonymous changes for (a) ACMV  
886 (blue) and (b) EACMCV (red). The number of synonymous (c) and non-synonymous (d) codon  
887 changes normalized to the total number of codons in the ORF for ACMV (dark grey and blue)  
888 and EACMCV (light grey and red). The number of synonymous (grey) and non-synonymous  
889 (ACMV-blue, EACMCV-red) codon changes in overlapping coding sequences in ORFs  
890 overlapping within ACMV excluding *AC5* (e), EACMCV (f), and regions within ACMV that  
891 overlap *AC5* (g). The overlapping ORF is designated first and the ORF assessed for the codon  
892 change is designated second in bold.

893 **Fig 5. ACMV common regions undergo sequence convergence.**

894 (a) Linear maps of ACMV DNA-A and ACMV DNA-B. The maps were linearized in the  
895 common region at the cleavage site in the top strand of the viral origin of replication. Red arrows  
896 mark the 3'-OH and the 5'-P of the nick site (99). The common region upstream (yellow) and  
897 downstream (grey) of the nick site are marked. The open reading frames and directions of  
898 transcription are shown by the black arrows below. (b) ACMV DNA-A and ACMV DNA-B  
899 sequences showing their common regions in the circularized genomic form. The labeling is the  
900 same as in (a), with the nick site indicated by a red arrow and the upstream and downstream  
901 sequences marked by yellow and grey shading, respectively. The iterons (boxed) and the hairpin  
902 motif (stem: underlined; loop: dotted line) involved for the initiation of viral replication are  
903 marked. The TATA box (underlined) for complementary sense transcription is also labeled.



904 SNPs showing convergence of the common region sequences of DNA-A and DNA-B are in  
905 black typeface, and other SNPs are in red typeface.

906 **Fig 6. EACMCV common regions undergo sequence convergence.**

907 (a) Linear maps of EACMCV DNA-A and EACMCV DNA-B. The maps were linearized in the  
908 common region at the cleavage site in the top strand of the viral origin of replication. Red arrows  
909 mark the 3'-OH and the 5'-P of the nick site (99). The common region upstream (yellow) and  
910 downstream (grey) of the nick site are marked. The open reading frames and directions of  
911 transcription are shown by the black arrows below. (b) EACMCV DNA-A and EACMCV DNA-  
912 B sequences showing their common regions in the circularized genomic form. The labeling is the  
913 same as in (a), with the nick site indicated by a red arrow and the upstream and downstream  
914 sequences marked by yellow and grey shading, respectively. The iterons (boxed) and the hairpin  
915 motif (stem: underlined; loop: dotted line) involved for the initiation of viral replication are  
916 marked. The TATA box (underlined) for complementary sense transcription is also labeled.  
917 SNPs showing convergence of the common region sequences of DNA-A and DNA-B are in  
918 black typeface, and other SNPs are in red typeface. Insertion is indicated by italics.

919

920 **SUPPLEMENTAL MATERIAL**

921 **S1. ACMV and EACMCV clones.** Diagram of A and B components of ACMV (a, b) and  
922 EACMCV (c, d). Black arrows represent opening reading frames, and the red arrow indicates  
923 nick site. (e) The table shows the gene name of each opening reading frame, the corresponding  
924 protein name, and function(s) of the protein in infection.

925 **S2. Veg6 ACMV nucleotide diversity sliding windows of all 7 rounds.** (a) Sliding window  
926 analysis of nucleotide diversity ( $\pi$ ) of ACMV DNA-A and DNA-B and (c) EACMCV DNA-A  
927 and DNA-B. Dark pink to dark green represents the nucleotide diversity across the genome of  
928 inoculated plants (P1) and six vegetative propagations (P2-P7). Enhanced views of the  
929 nucleotide diversity of the *AVI* and *ACI* open reading frames during P1-P7 for ACMV-A (b) and  
930 EACMCV-A (d). Blue lines mark the locations of codons encoding functional motifs in the Rep  
931 protein, i.e. Rep C, Rep B, Walker B, Walker A (63), Motif 3 (62), GRS (64), Motif 2 (62) and  
932 Motif 1 (82). The motifs are shown to scale. Genome coordinates (nt), the positions of open  
933 reading frames and their directions of transcription are shown below each graph.

934 **S3. Supplementary Tables 1-7.**

935 Table S3-1. Veg6 full experimental model ANOVA results.

936 Table S3-2. Full experimental model ANOVA results for Veg2 experiment.

937 Table S3-3.  $\chi^2$  analysis of the number of coding regions at a genome position and codon  
938 changes.

939 Table S3-4. Analysis of nucleotide substitution bias in the Veg2 and Veg6 experiments.

940 Table S3-5. Nucleotide changes at a frequency >3% in multiple passages in the Veg2  
941 experiment.



942 Table S3-6. Nucleotide changes at a frequency >3% in multiple passages in the Veg6  
943 experiment.

944 Table S3-7. Veg6 nucleotide changes present in the historical database.

945 Table S3-8. Mann-Whitney test results between frequency of SNPs in Veg6 and those found in  
946 the historical database.

947

948

Fig. 1 Aimone and Lavington et al

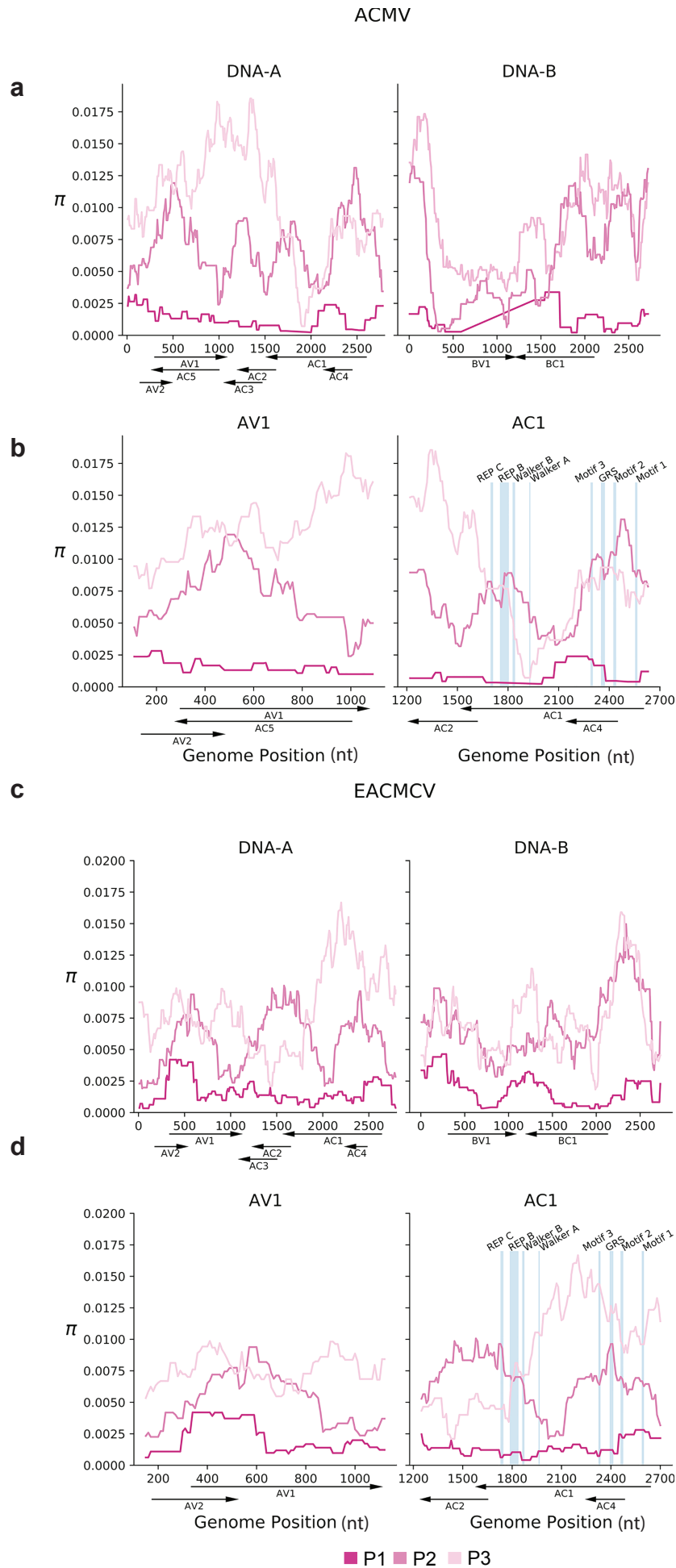


Fig. 2 Aimone and Lavington et al

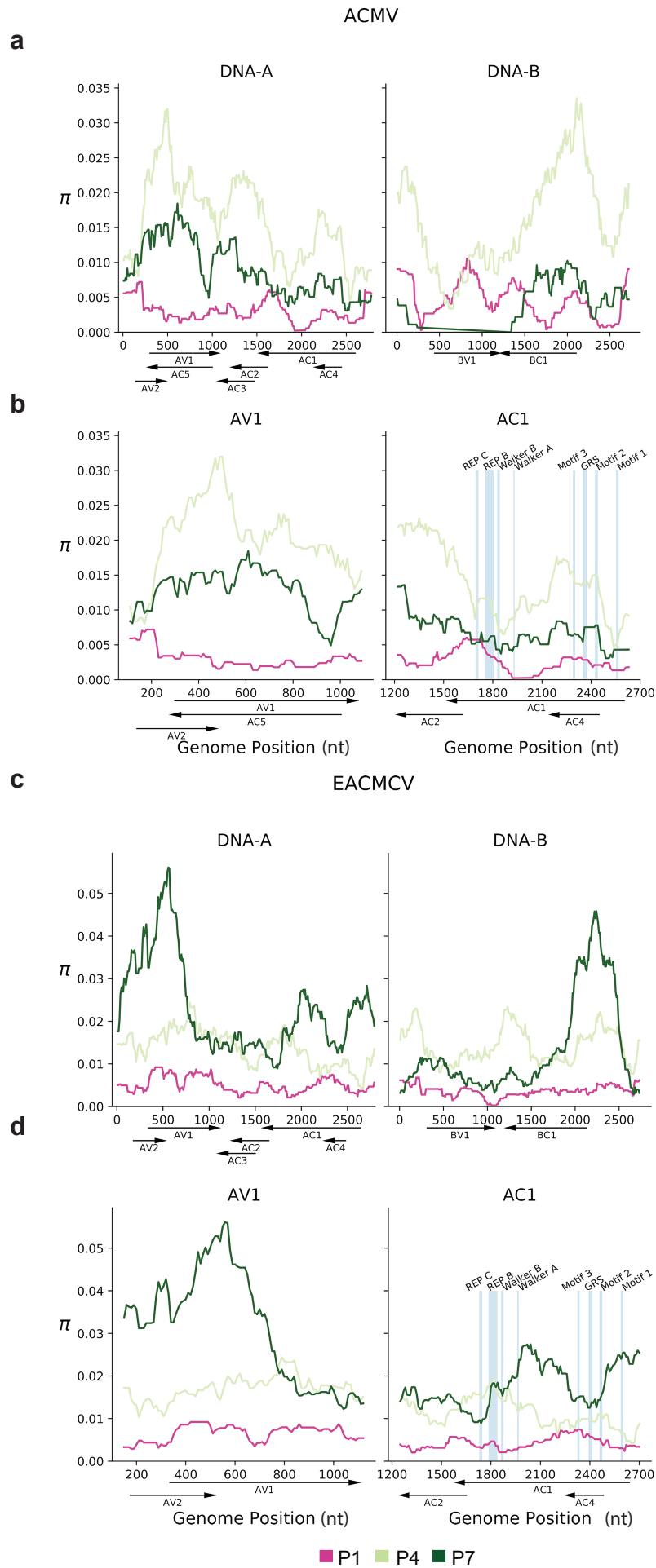


Fig.3 Aimone and Lavington et al

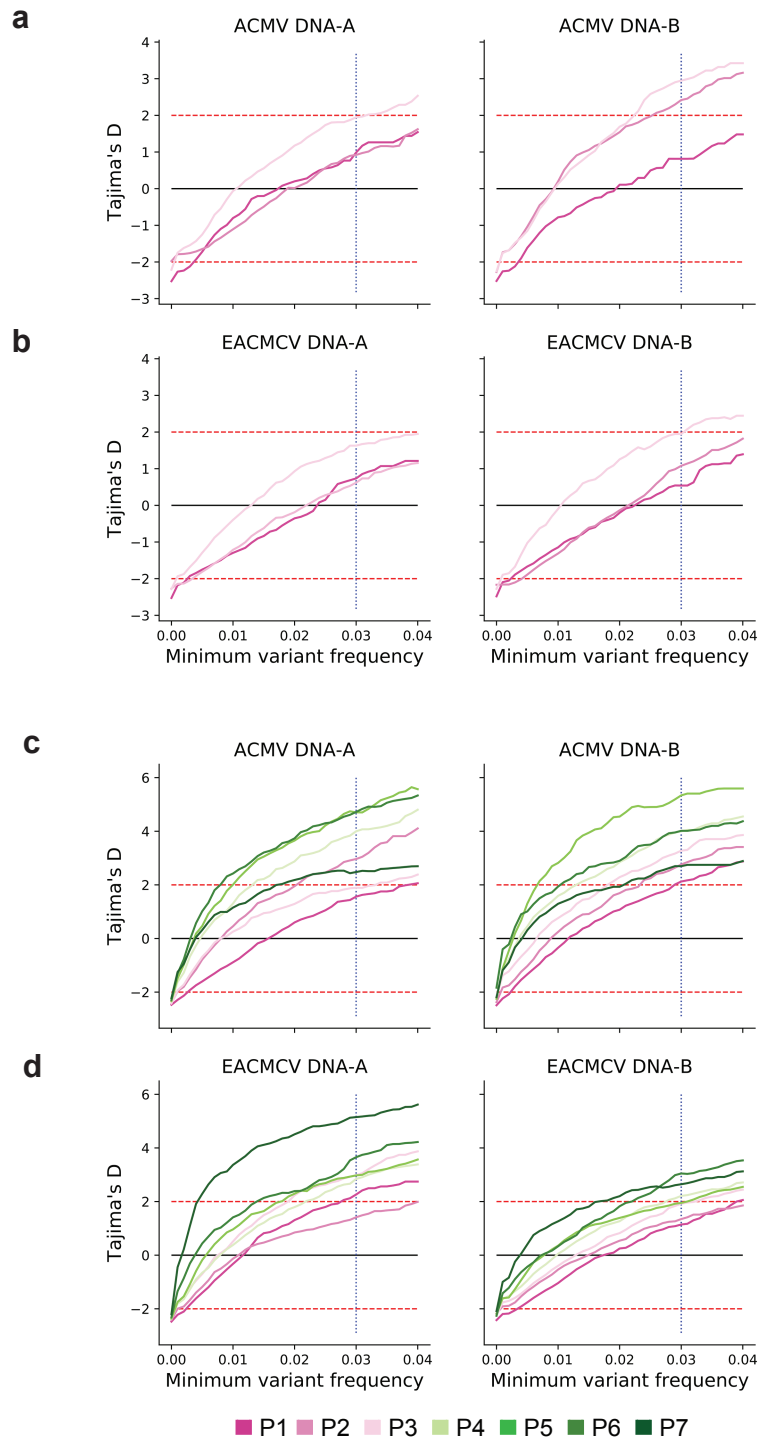


Fig. 4 Aimone and Lavington et al

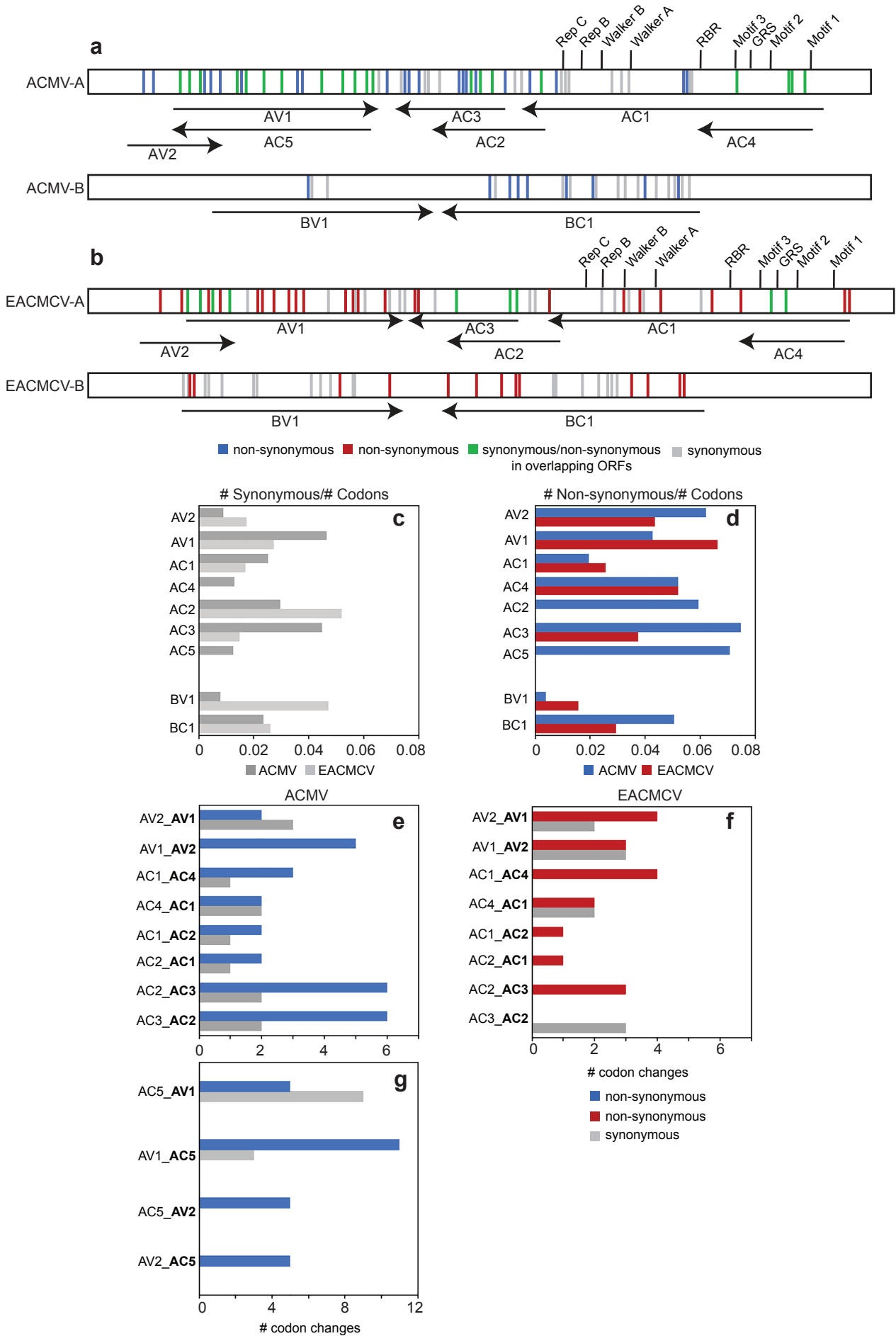


Fig. 5 Aimone and Lavington et al

